Supporting Information

An AIE Molecule Featured with Changeable Triplet Emission between Phosphorescence and Delayed Fluorescence by External force

Lili Huang,[ac] Xue Wen,[ac] Jianwei Liu,[a] Mingxing Chen,[b] Zhiyong Ma[a]* and Xinru Jia[b]

1. Materials and General Methods

All the solvents and reactants were purchased from commercialized companies and used as received without further purification except for specifying otherwise.

^{1}H NMR was recorded on the 400 MHz (Bruker ARX400) and ^{13}C NMR spectra were recorded on the Bruker 125 MHz spectrometer at room temperature with $CDCl_3$ as the solvent and tetramethylsilane (TMS) as the internal standard. ESI high resolution mass-spectra (HRMS) were acquired on a Bruker Apex IV FTMS mass spectrometer. UV-Vis spectra were acquired on the Hitachi U-3900H UV-vis spectrophotometer. Transient and delayed photoluminescence spectra were performed on the Hitachi F-4600 or Edinburgh Instruments FLS920 fluorescence spectrophotometer. Luminescence lifetime were acquired on the Lifespec-Red Picosecond Lifetime Spectrometer or Edinburgh Instruments FLS980 fluorescence spectrophotometer (λ_{ex}=375nm). Differential scanning calorimetry (DSC) measurement was carried out by using TA instruments Q100 DSC. Wide-angle X-ray diffraction (WAXD) experiments were performed on a Philips X'PertPro diffractometer with a 3 kW ceramic tube as the X-ray source (Cu Kα) and an X'celerator detector. Single crystal X-ray diffraction data were collected with a NONIUS KappaCCD diffractometer with graphite monochromator and Mo Kα radiation [λ (MoKα) = 0.71073 Å]. Structures were solved by direct methods with SHELXS-97 and refined against F2 with SHELXS-97.

TD-DFT calculations were conducted on Gaussian 09 program with a method similar to previous

literature. [1] Ground state (S0) geometries of ImF and ImBr were directly selected from single crystal structures and were used as molecular models without further optimization. On the basis of this, exciton energies in singlet (Sn) and triplet states (Tn) were estimated through a combination of TDDFT and B3LYP at the 6-311+G(p, d) level. Kohn-Sham frontier orbital analysis was subsequently performed based on the results of theoretical calculation to elucidate the mechanisms of possible singlet-triplet intersystem crossings, in which the channels from S1 to Tn are believed to share part of the same transition orbital compositions. Herein, energy levels of the possible Tn states are considered to lie within the range of *E*S1±0.3 eV. [2]

2. Synthetic route to ODFRPTZ

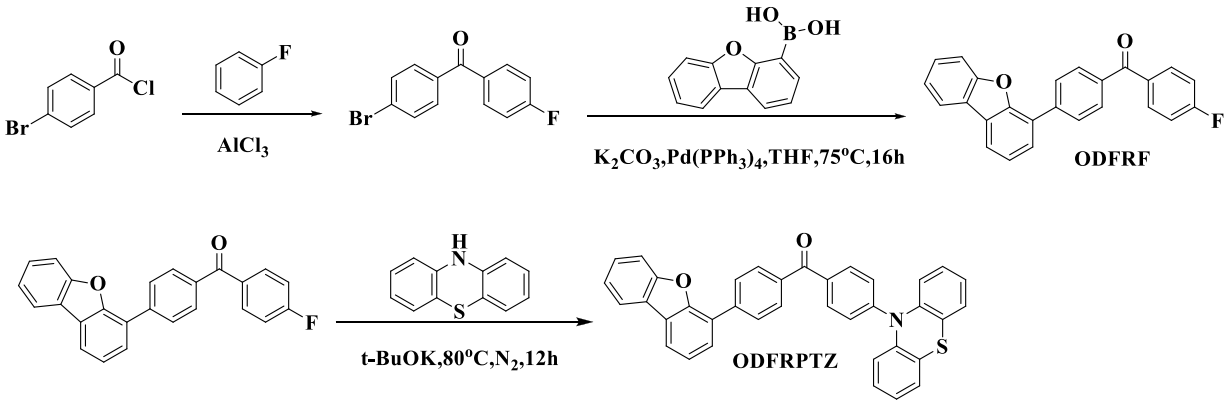

Scheme S1. The synthetic routes to ODFRPTZ.

Synthesis of 4-Bromo-4'-fluorobenzophenone

OFBr was prepared according to the previous work. [3] Firstly, to a schlenk flask, anhydrous $AlCl_3$ (1.80 g, 6 mmol) and 4-Bromobenzoyl chloride (1.10 g, 5 mmol) was added. After being degased and refilled with nitrogen for three cycles, 20 ml fluorobenzene was slowly injected at 0 °C. The reaction mixture was stirred at room temperature for 30 min, refluxed overnight and again stirred at room temperature for 4h. The resulting reaction was poured into 50 ml 5 M HCl and was extracted with dichloromethane for three times. After being dried over anhydrous $NaSO_4$ and concentrated by rotary

evaporation, the residue was purified by recrystallization in petroleum ether/ethanol mixed solution to get the pure white production. The yield is 88%.

^{1}H NMR (400 MHz, $CDCl_3$) δ = 7.85 (dd, *J*=8.5, 5.5, 2H), 7.67 (s, 4H), 7.20 (t, *J*=8.5, 2H).

HR-ESI-MS Calcd. For $C_{13}H_9BrFO$ $[M+H]^+$: 278.981532. Found: 278.98123.

Synthesis of ODFRF

The Suzuki–Miyaura coupling reaction was done referring to the previous work.[4] OFBr (976.9 mg, 3.5 mmol), dibenzofuran (848 mg, 4 mmol), K_2CO_3(1105.7mg,8mmol) and $Pd(PPh_3)_4$ were sequentially added to a schlenk flask； 15 mL THF of HPLC grade and 5 mL degassed deionized water was injected under nitrogen. The solution was refluxed at 75 ºC for 16h. After removing the solvent under reduced pressure, the pure white product ODFRF was obtained by column chromatography with silica gel (DCM: petroleum ether=1:1 as the eluent). Yield: 85%.

^{1}H NMR (400 MHz, $CDCl_3$) δ = 8.06 (d, *J*=8.3, 2H), 8.03 – 7.98 (m, 2H), 7.97 – 7.90 (m, 4H), 7.64 (dd, *J*=17.0, 7.9, 2H), 7.51 – 7.44 (m, 2H), 7.38 (t, *J*=7.4, 1H), 7.20 (t, *J*=8.6, 2H).

^{13}C NMR (101 MHz, $CDCl_3$) δ = 206.94 (s), 194.86 (s), 166.68 (s), 164.16 (s), 156.18 (s), 153.36 (s), 140.68 (s), 136.49 (s), 133.96 (d, *J* = 3.1 Hz), 132.68 (d, *J* = 9.2 Hz), 130.36 (s), 128.70 (s), 127.50 (s), 126.85 (s), 125.23 (s), 124.56 (s), 124.01 (s), 123.39 (s), 123.03 (s), 120.73 (d, *J* = 12.4 Hz), 115.63 (s), 115.42 (s), 111.87 (s).

HR-ESI-MS Calcd. For $C_{25}H_{16}FO_2$ $[M+H]^+$: 367.112884. Found: 367.11298.

Synthesis of ODFRPTZ

ODFRF (600.9 mg, 1.64 mmol), carbazole (2.2 mmol, 367.9 mg) and potassium were added to a schlenk flask. After injecting 15 ml N,N-Dimethylformamide, the mixture was stirred at room temperature for 15 min under nitrogen. Then tert-butoxide (3 mmol, 336.6 mg) dissolved in DMF was injected and the solution was refluxed at 110 ºC overnight. The resulting solution was cooled down to room temperature, poured into ice water and extracted with dichloromethane. After being concentrated in vacuum, ODFRPTZ was gained by column chromatography with silica gel (DCM: petroleum ether=1:1 as the eluent). Yield: 83%.

^{1}H NMR (400 MHz, CDCl3) δ=8.08 (d, J = 8.4 Hz, 2H), 8.05 – 7.99 (m, 4H), 7.96 (d, J = 8.7 Hz, 2H), 7.72 – 7.62 (m, 2H), 7.56 – 7.48 (m, 2H), 7.42 (dd, J = 10.9, 4.0 Hz, 1H), 7.38 – 7.30 (m, 4H), 7.22 (td, J = 7.8, 1.5 Hz, 2H), 7.12 (td, J = 7.5, 1.2 Hz, 2H), 7.05 (dd, J = 8.0, 1.0 Hz, 2H).

^{13}C NMR (101 MHz, CDCl3) δ = 194.97 (s), 156.20 (s), 153.38 (s), 147.72 (s), 142.20 (s), 140.32 (s), 136.99 (s), 132.86 (s), 132.39 (s), 130.32 (s), 129.04 (s), 128.64 (s), 128.41 (d, J=44.2), 127.48 (s), 127.20 (s), 126.88 (s), 125.10 (d, J=21.1), 124.72 (s), 124.05 (s), 123.38 (s), 122.92 (d, J=16.4), 120.68 (d, J=21.8), 120.55 – 120.39 (m), 111.89 (s).

HR-ESI-MS Calcd. For $C_{37}H_{23}NO_2S$ $[M+H]^+$: 546.152227. Found: 546.15284.

3. NMR spectra and HR-MS of ODFRPTZ

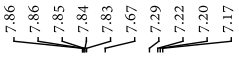

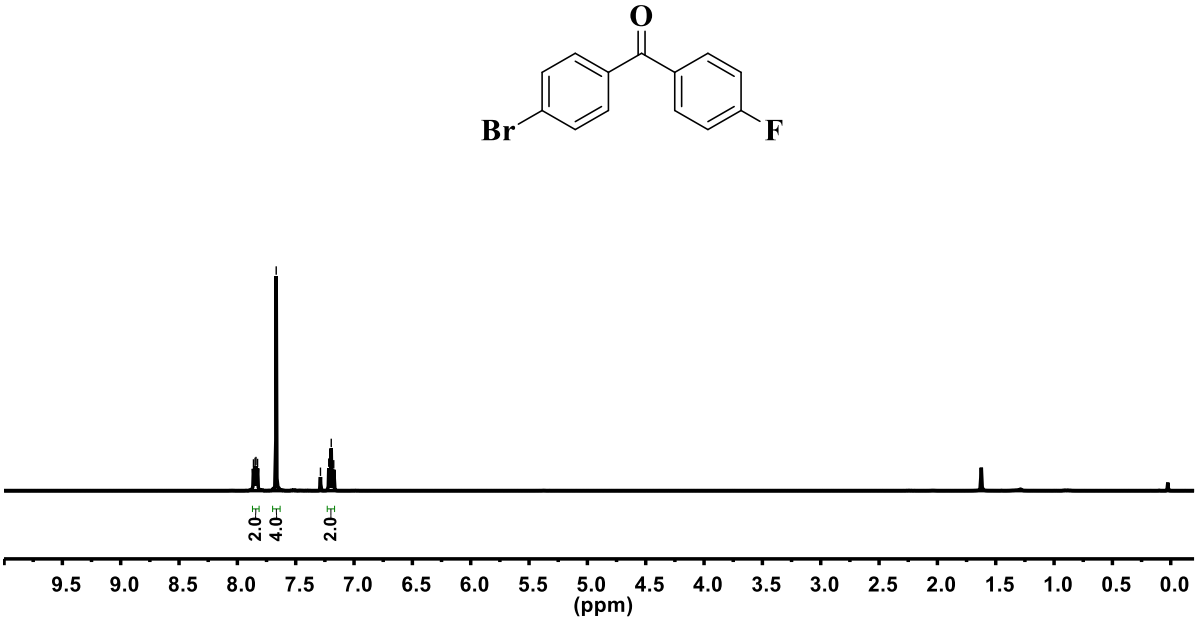

Figure S1. ^{1}H NMR spectrum of **OFBr** in $CDCl_3$.

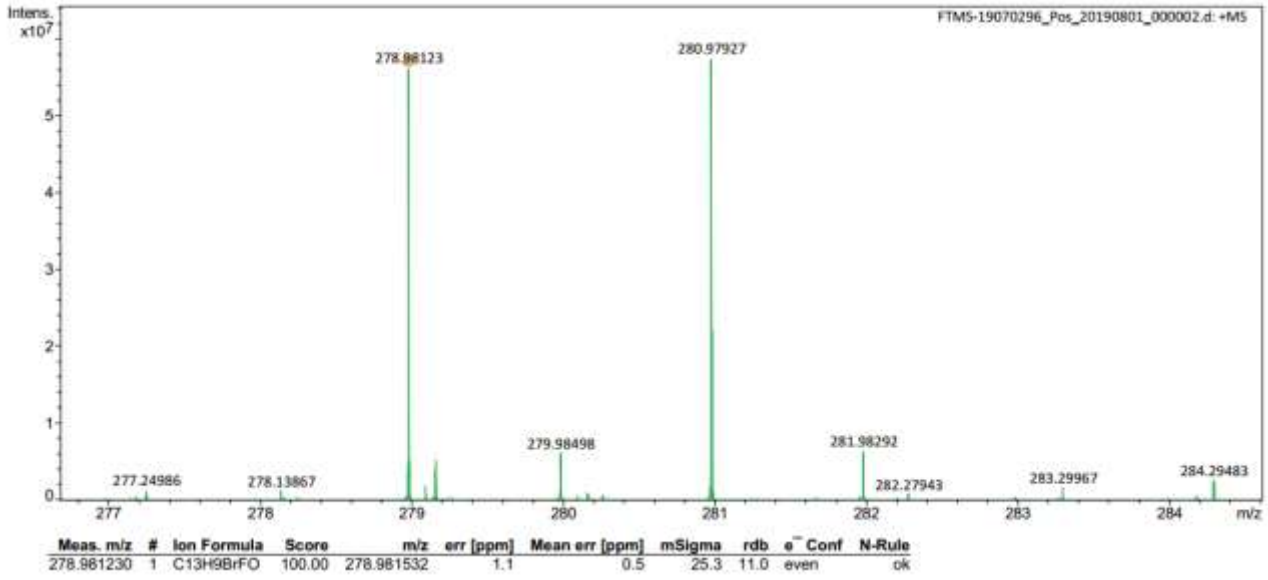

Figure S2. HR-MS spectrum of **OFBr**.

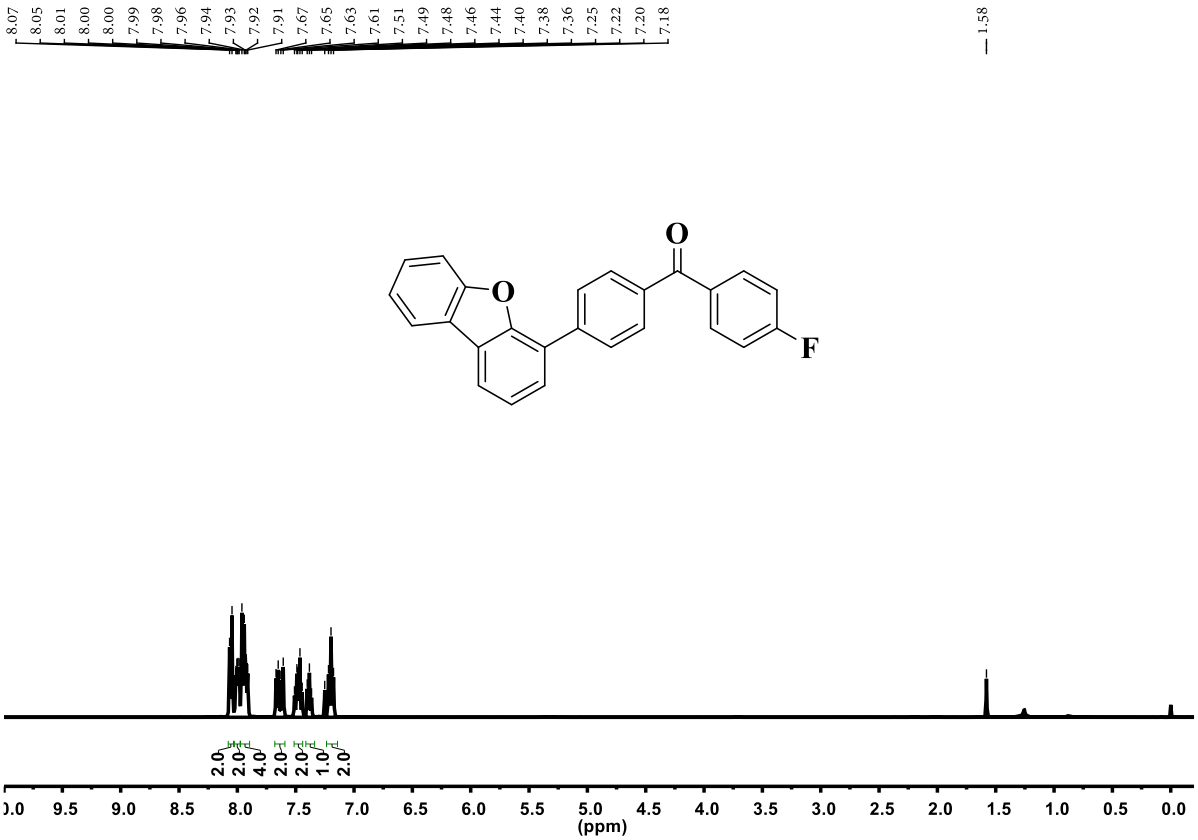

Figure S3. ^{1}H NMR spectrum of **ODFRF** in $CDCl_3$.

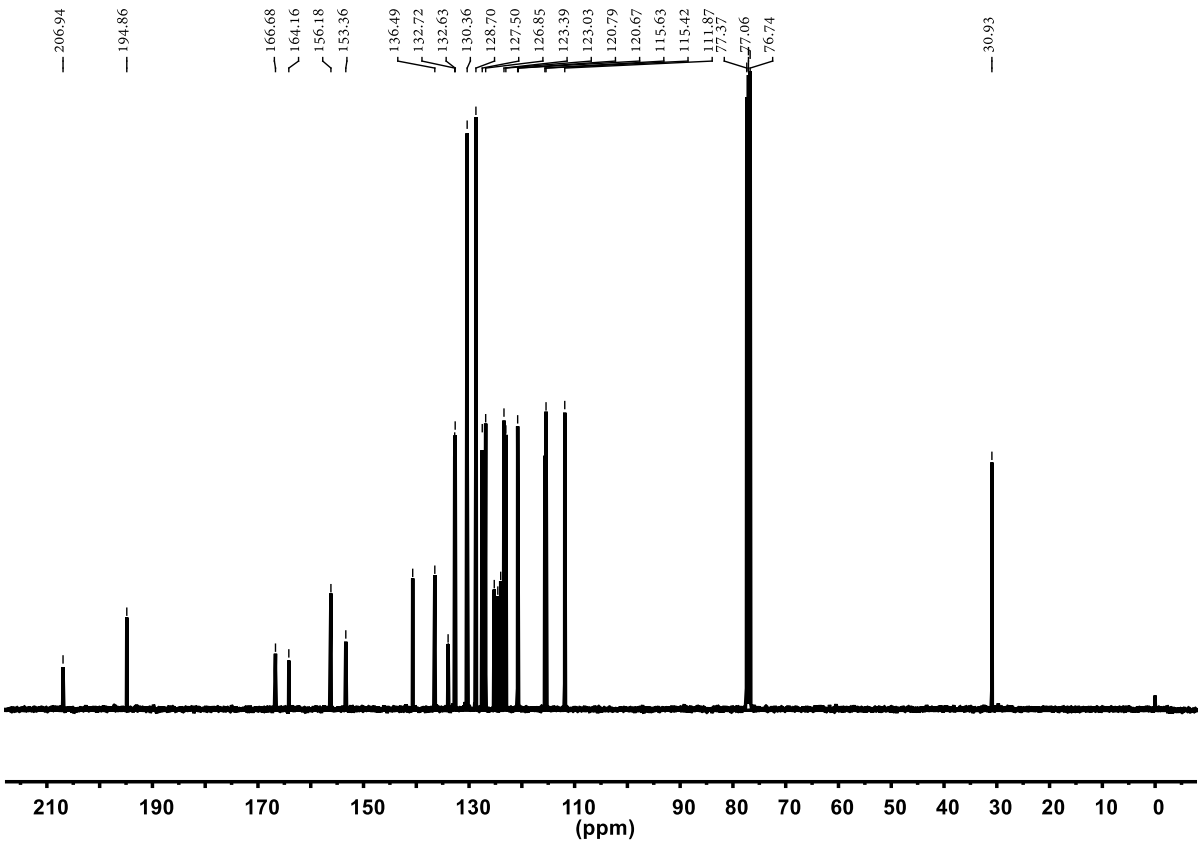

Figure S4. ^{13}C NMR spectrum of **ODFRF** in $CDCl_3$ (The peak at 30.93 ppm is the signal of petroleum ether from the eluting solvent.).

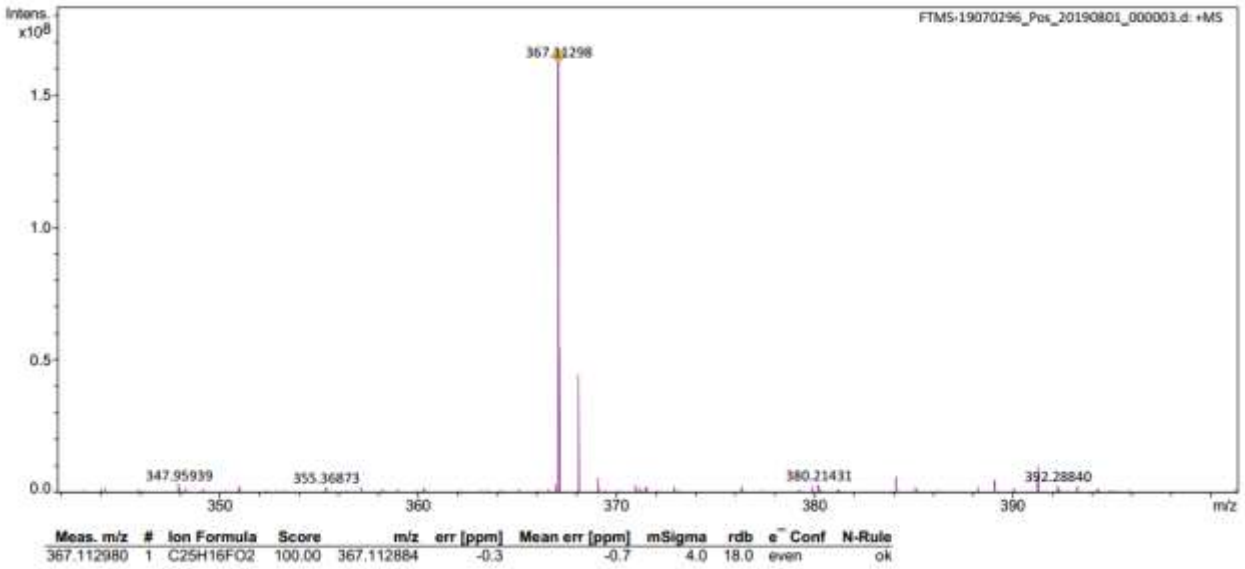

Figure S5. HR-MS spectrum of **ODFRF**.

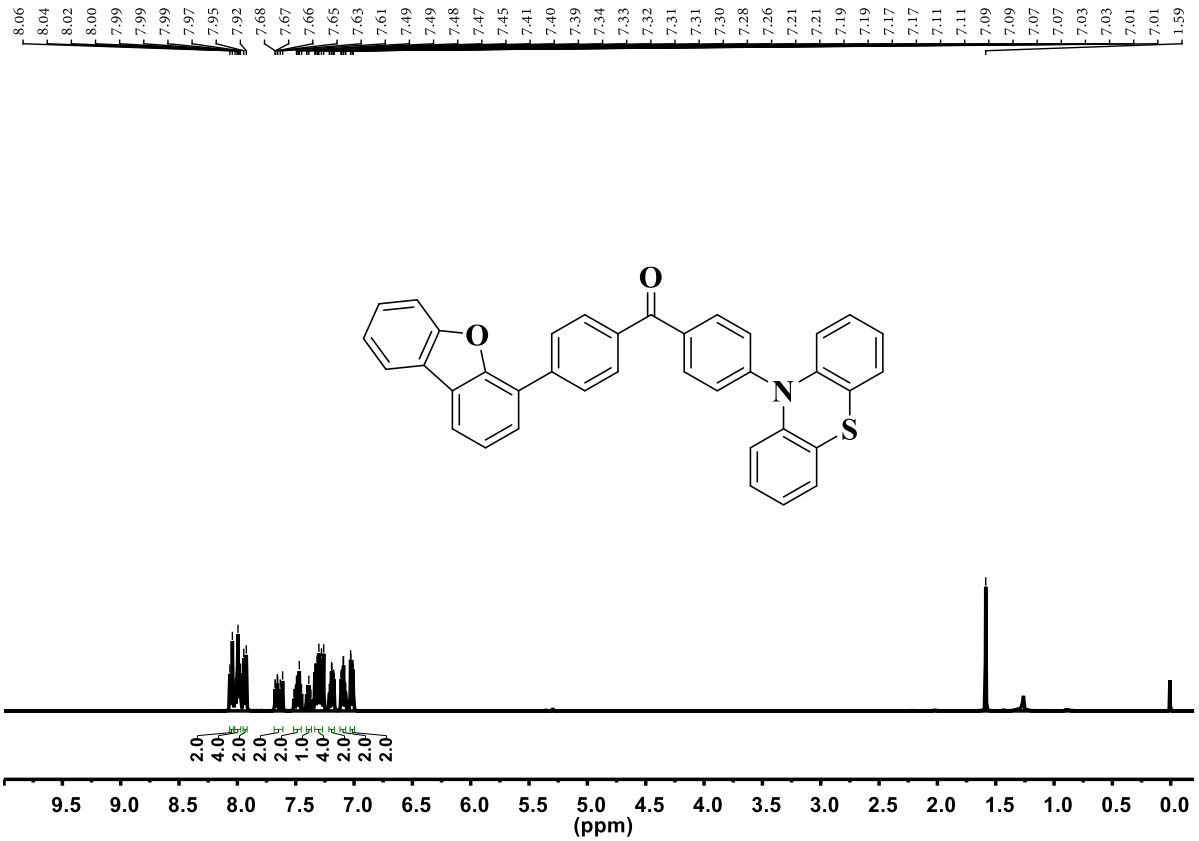

Figure S6. ^{1}H NMR spectrum of **ODFRPTZ** in $CDCl_3$ (the peak at 1.55 ppm is the signal of H_2O from the $CDCl_3$ solvent; the peak at 1.25 ppm is the signal of petroleum ether from the eluting solvent.).

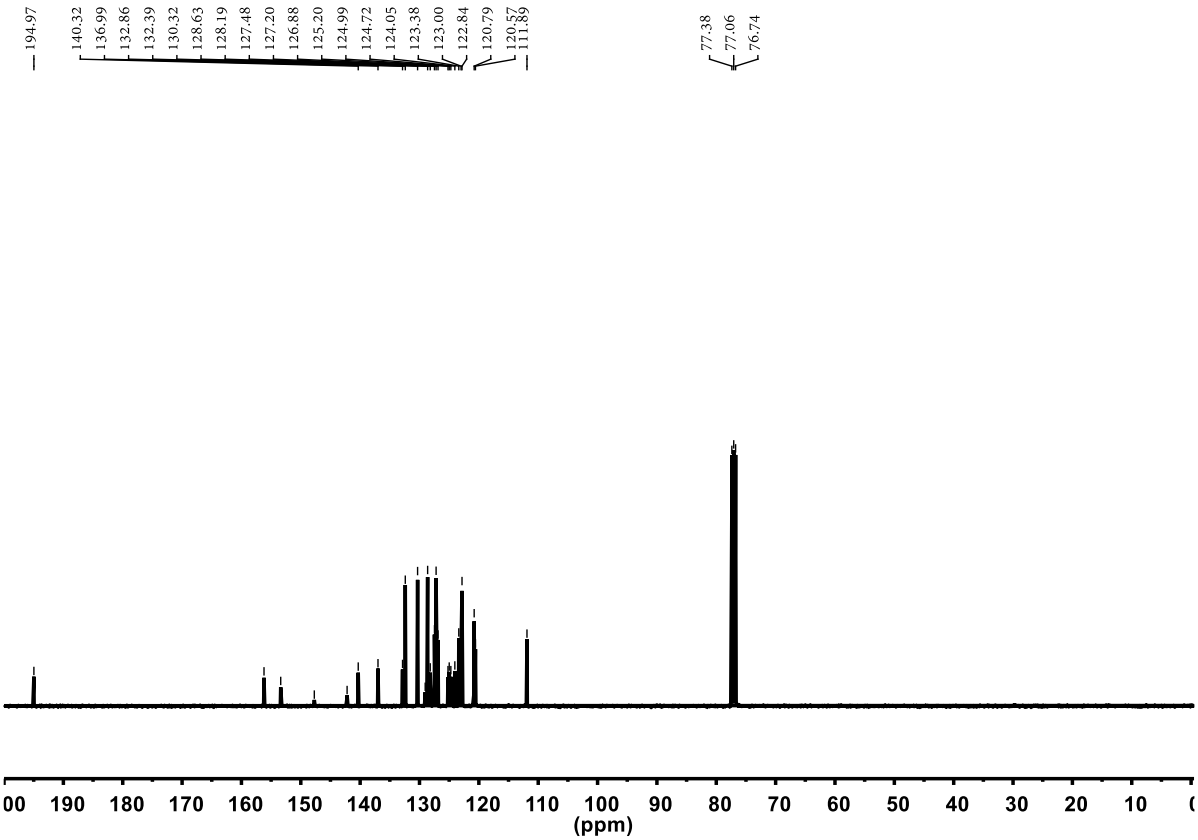

Figure S7. ^{13}C NMR spectrum of **ODFRPTZ** in $CDCl_3$.

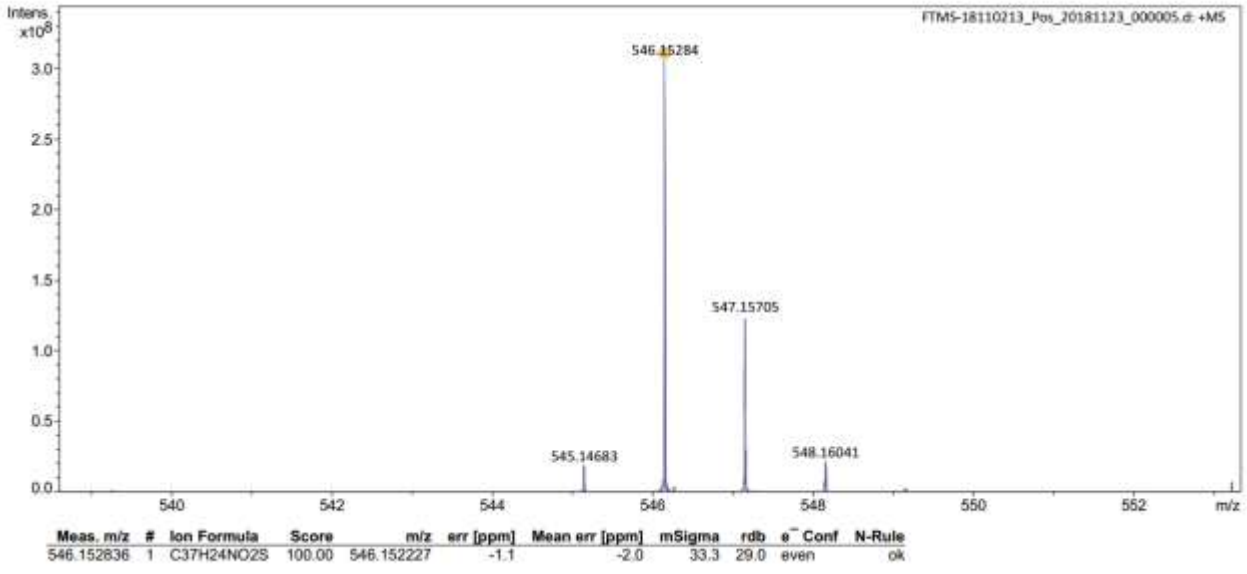

Figure S8. HR-MS spectrum of **ODFRPTZ**.

4. Absorption spectrum of the solid powder

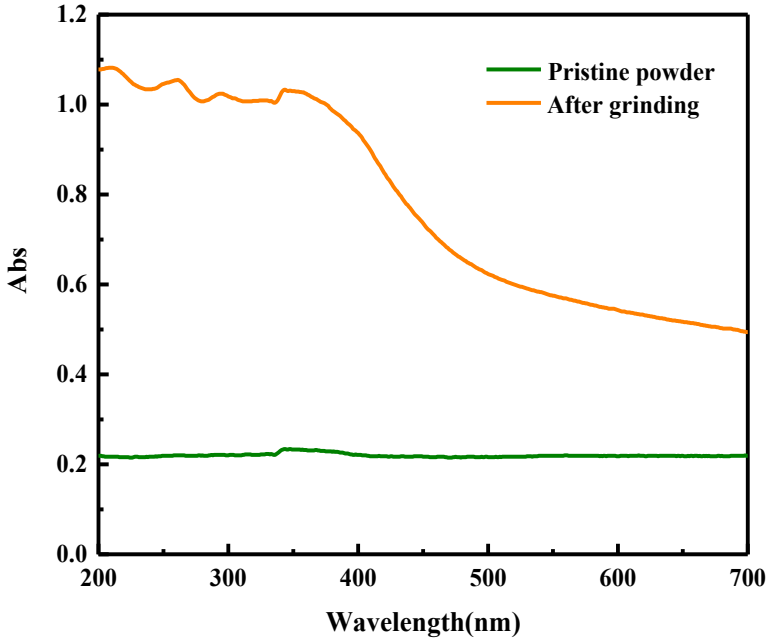

Figure S9. Absorption spectrum of pristine and ground powder of ODFRPTZ.

5. Reversible mechanochromic property of ODFRPTZ

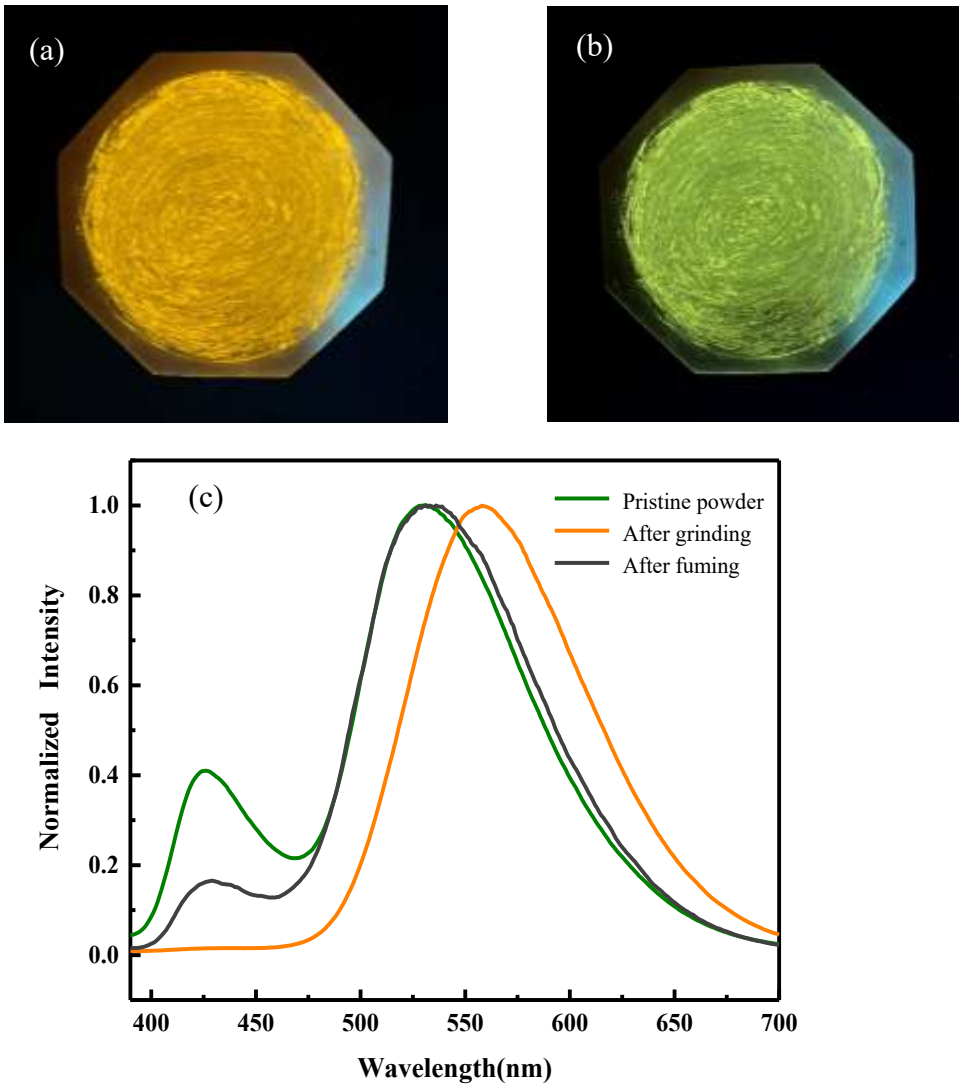

Figure S10. Optical images of ground ODFRPTZ powder under 365 nm UV light (a) before and (b) after fuming. (c) Fluorescence spectra of original powder, ground powder and recovered powder after fuming.

6. DSC curves

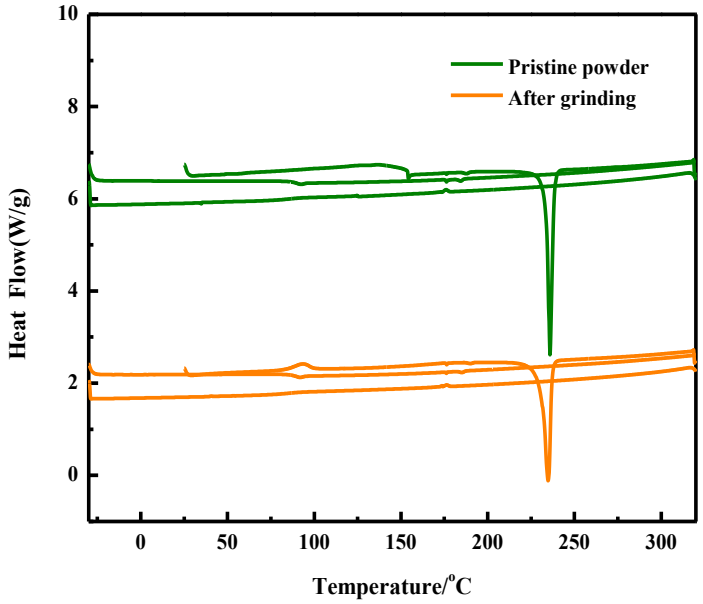

Figure S11. DSC curves of the pristine ODFRPTZ powder and the ground one.

7. Decay curve of the prompt fluorescence at 540 nm

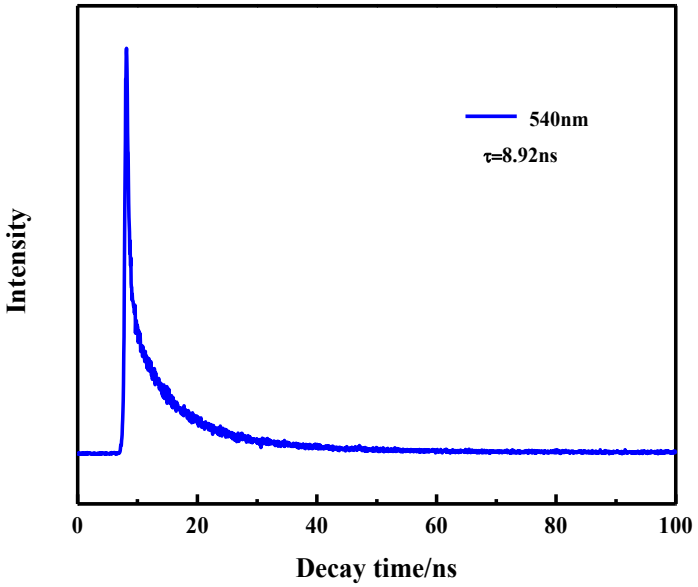

Figure S12. Decay curve of the prompt fluorescence at 540 nm.

8. Detailed data of ODFRPTZ single crystal

Table S1. Detailed data of **ODFRPTZ** single crystal.

Identification code	ODFRPTZ
CCDC Number	1902888
Empirical formula	$C_{37}H_{23}N\ O_2S$
Formula weight	545.62
Temperature	297 K
Wavelength	0.71073 Å
Crystal system	triclinic
Space group	P-1
Unit cell dimensions	a = 8.9754(4) Å, α= 111.039(2).
	b = 11.9049(6) Å, β= 90.487(2).
	c = 13.8094(7) Å, γ = 95.955(2).
Volume	1368.09(12) $Å^3$
Z	2
Density (calculated)	1.325 Mg/m^3
Absorption coefficient	0.154 mm^{-1}
F(000)	568
Theta range for data collection	2.833 to 27.526°.
Index ranges	-11=h<=11, -15<=k<=15, -17<=l<=17
Reflections collected	37658
Independent reflections	4733 [R(int) = 0.951]
Final R indices [I>2sigma(I)]	R1 =0.0849, wR2 = 0.1496
R indices (all data)	R1 = 0.1058, wR2 = 0.1566

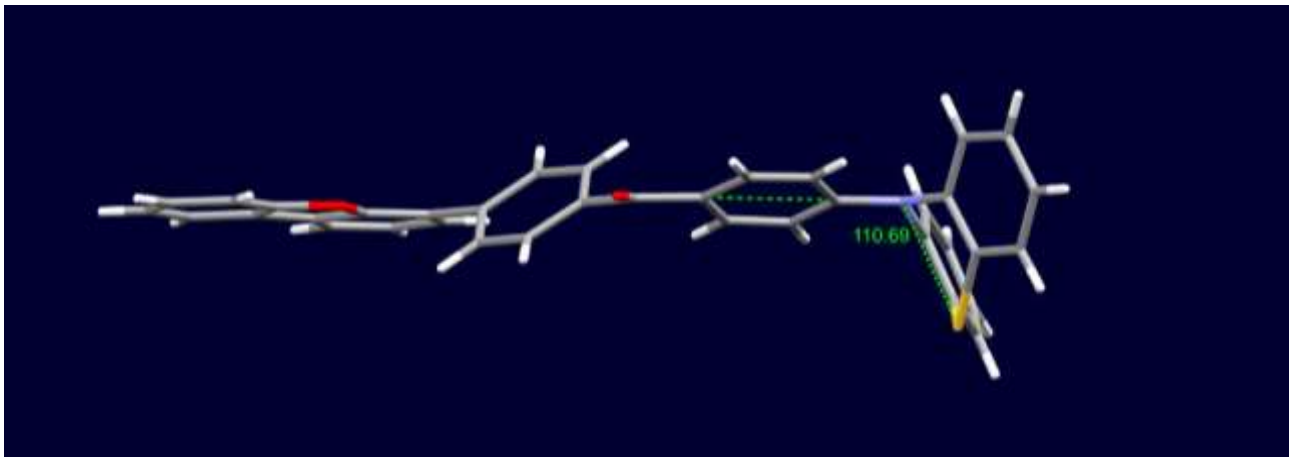

Figure S13. The "quasi-axial" conformation of ODFRPTZ with a dihedral angle of 110.7° in the unit cell.

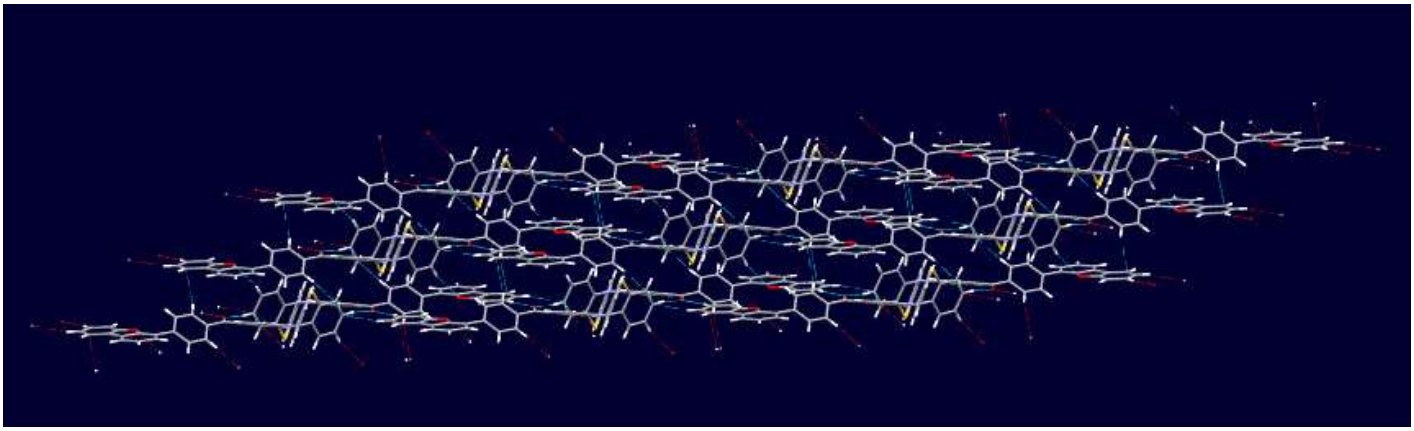

Figure S14. Layer-by-layer structure of ODFRPTZ in the single crystal.

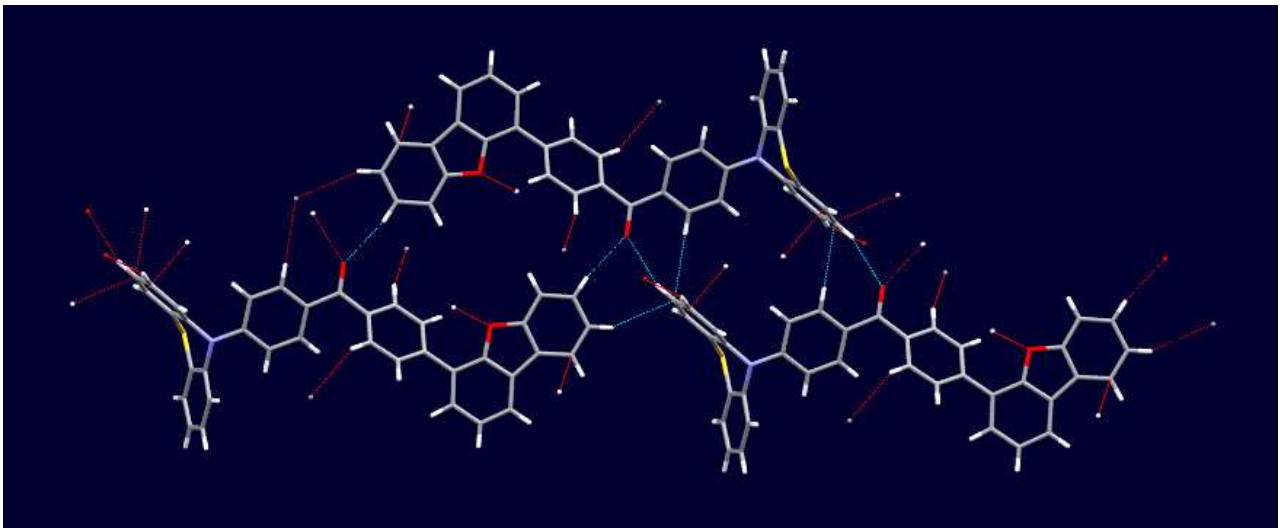

Figure 15. The firm interactions between any two of dibenzofuran, phenothiazine and carbonyl subunits.

9. TD-DFT results

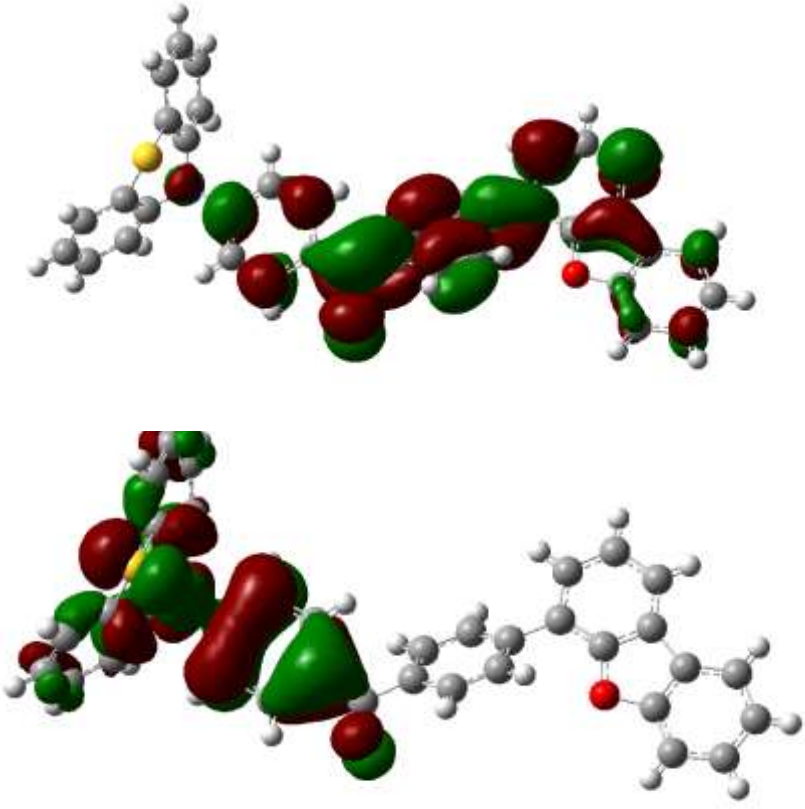

Figure 16. The LUMO (up) and HOMO (down) of ODFRPTZ based on the single crystal data.

Table S2. Triplet excited states of ODFRCZ that contain the same orbital transition components of S1.

Excited State	Energy (eV)	Transition configuration (%)
Monomer		
T1	2.8844	H→L(40.9%), H-1→L(17.4%), H-4→L(8.6%)
T2	3.0194	H→L(17.8%), H-1→L(42.5%), H-4→L(2.1%)
T3	3.2104	H→L(4.0%), H-4→L+1(5.4%), H-4→L(42.6%), H-5→L(3.1%)
T4	3.3846	H-1→L(7.6%), H-4→L(10.7%), H-5→L(7.4%)
T5	3.5609	-
T6	3.6133	-
S1	**3.6133**	**H→L(23.9%), H-1→L(8.4%), H-4→L+1(7.2%), H-4→L(45.1%), H-5→L(4.5%), H-6→L(2.4%)**
S2	**3.6617**	**-**
T7	3.6989	H-4→L+1(5.6%), H-5→L(17.3%)
T8	3.8004	-
T9	3.8506	H→L(3.2%)
T10	3.9481	H→L(29.9%)
Dimer 1		
T1	2.8409	H→L(15.3%), H-1→L+1(15.7%)
T2	2.8410	H→L(12.4%), H-1→L+1(10.9%)
T3	3.0048	-
T4	3.0050	-
T5	3.2432	-
T6	3.2434	-
T7	3.3975	-
T8	3.3976	-
S1	**3.5054**	**H→L(50.3%), H-1→L+1(42.5%)**
S2	**3.5278**	**-**
T9	3.5643	-
T10	3.5648	-
T11	3.6126	H→L(8.3%)
T12	3.6131	H→L(34.3%), H-1→L+1(51.5%)
T13	3.6137	H→L(30.4%), H-1→L+1(17.5%)
T14	3.6139	H→L(10.8%), H-1→L+1(21.7%)
T15	3.6348	H→L(9.9%), H-1→L+1(8.0%)
T16	3.6352	-
T17	3.6864	-
T18	3.6887	H→L(3.6%)
T19	3.7024	

Dimer 2		
T1	2.8948	H→L+1(21.8%), H-1→L(22.9%), H-2→L(7.2%)
T2	2.8950	-
T3	3.0027	-
T4	3.0028	H→L+1(12.2%), H-1→L(10.7%), H-2→L(17.4%)
T5	3.2339	H-1→L(2.1%)
T6	3.2342	-
T7	3.3779	-
T8	3.3785	-
T9	3.5624	-
T10	3.5624	-
T11	3.6145	-
T12	3.6145	-
S1	**3.6500**	**H→L+1(42.0%), H-1→L(47.0%), H-2→L(2.1%)**
S2	**3.6591**	-
S3	**3.6675**	-
S4	**3.6680**	-
T13	3.7076	-
T14	3.7080	-
T15	3.8105	-
T16	3.8105	-
T17	3.8248	-
T18	3.8249	H-2→L(11.0%)
T19	3.8605	-
T20	3.8606	-

10. Decay curve of the prompt fluorescence at 581 nm

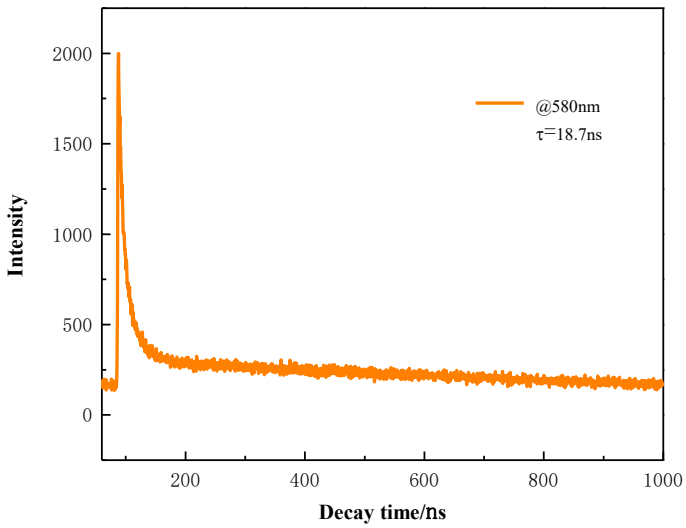

Figure S17. Decay curve of the prompt fluorescence at 581 nm.

References

[1] L. Jian-An, Z. Jinghong, M. Zhu, X. Zongliang, Y. Zhan, X. Bingjia, L. Cong, C. Xin, R. Dingyang, P. Hui, S. Guang, Z. Yi, C. Zhenguo, *Angew. Chem. Int. Ed.* **2018**, *57*, 6449-6453.

[2] Z. An, C. Zheng, Y. Tao, R. Chen, H. Shi, T. Chen, Z. Wang, H. Li, R. Deng, X. Liu, W. Huang, *Nat. Mater.* **2015**, *14*, 685-690.

[3] Y. Du, N. Dong, M. Zhang, B. Jiang, N. Sun, Y. Luo, S. Zhang, G. Wang, J. Wang, *J. Mater. Chem. C* 2018, **6**, 7317.

[4] B. Xu, H. Wu, J. Chen, Z. Yang, Z. Yang, Y. C. Wu, Y. Zhang, C. Jin, P. Y. Lu, Z. Chi, *Chem. Sci.* **2017**, *8*, 1909.